

Trk retrograde signaling requires persistent, Pincher-directed endosomes

Polyxeni Philippidou^{a,1}, Gregorio Valdez^{a,2}, Wendy Akmentin^a, William J. Bowers^b, Howard J. Federoff^c, and Simon Halegoua^{a,3}

^aDepartment of Neurobiology and Behavior, Center for Nervous System Disorders and Program in Neuroscience, Stony Brook University, Stony Brook, NY 11794-5230; ^bDepartments of Neurology, Microbiology, and Immunology, and Pharmacology and Physiology, Center for Neural Development and Disease, University of Rochester Medical Center, Rochester, NY 14642; and ^cDepartment of Neurology, Georgetown University Medical Center, Washington, DC 20057

Edited* by Gail Mandel, The Howard Hughes Medical Institute, Oregon Health and Science University, Portland, OR, and approved December 9, 2010 (received for review October 26, 2010)

Target-derived neurotrophins use retrogradely transported Trk-signaling endosomes to promote survival and neuronal phenotype at the soma. Despite their critical role in neurotrophin signaling, the nature and molecular composition of these endosomes remain largely unknown, the result of an inability to specifically identify the retrograde signaling entity. Using EGF-bound nanoparticles and chimeric, EGF-binding TrkB receptors, we elucidate Trk-endosomal events involving their formation, processing, retrograde transport, and somal signaling in sympathetic neurons. By comparing retrograde endosomal signaling by Trk to the related but poorly neuromodulatory EGF-receptor, we find that Trk and EGF-receptor endosomes are formed and processed by distinct mechanisms. Surprisingly, Trk and EGF-receptors are both retrogradely transported to the soma in multivesicular bodies. However, only the Trk-multivesicular bodies rely on Pincher-dependent macroendocytosis and processing. Retrograde signaling through Pincher-generated Trk-multivesicular bodies is distinctively refractory to signal termination by lysosomal processing, resulting in sustained somal signaling and neuronal gene expression.

epidermal growth factor receptor | Erk kinase | *vgf*

Target-derived neurotrophins (NTs) promote the survival of innervating neurons during development and regulate neuronal phenotype throughout life (1). NT signaling is initiated at the nerve terminal and conveyed to the soma over long distances and time spans. In the widely accepted endosomal model for retrograde axonal signaling (2), NT-activated Trk receptors are endocytosed and retrogradely transported to the soma (3, 4). Sustained Trk tyrosine kinase-mediated signaling, through for example the Erk kinases, would then be necessary to mediate long-term changes in gene expression. However, long-lived signaling endosomes are counter to the classic role of endocytosis in receptor down-regulation. This finding is particularly true for the closely-related receptor tyrosine kinase, EGF receptor (EGFR), whose short endosomal lifetime results in transient signaling of Erk kinases that is insufficient to mediate long-term gene expression changes (5). This classic mode of clathrin-dependent, receptor-mediated endocytosis, which generates endosomes that are rapidly targeted for recycling or lysosomal degradation, would thus be unsuitable for retrograde NT signaling. One alternate mechanism for Trk is macroendocytosis, mediated by the EH-domain, dynamin-like ATPase, Pincher/EHD4 (6) and the small G protein, Rac, which results in sustained endosomal signaling (5, 7, 8). Pincher-mediated Trk endosomes and clathrin-mediated EGFR endosomes are differentially processed, resulting in a relatively delayed transition of Trk endosomes to Rab7-dependent lysosomal breakdown (5).

Despite evidence for retrograde signaling endosomes (2, 9), characterizing their nature and composition has been insufficient and controversial. Controversies over the endosome ultrastructure, the signaling components used [e.g., Erk5 (10) or Erk1/2 (11)], and the molecules involved in endosome processing and

transport [e.g., Rab5 (12) or Rab7 (13)] have yet to be resolved. A major stumbling block has been identifying a Trk-specific endosome. For example, using tagged-NGF, retrogradely transported NGF was ultrastructurally seen in small vesicles [NGF-Qdot (12), smooth endoplasmic reticulum (NGF-HRP) (14), multivesicular bodies (MVBs) and lysosomes (¹²⁵I-NGF or NGF-HRP (14, 15))]. This complexity may reflect not only the heterogeneity of endosomal populations but also the existence of two receptors for NGF, p75NTR and TrkA, which are internalized, processed, and transported in both distinct (16, 17) and overlapping (13) endosomal compartments. We establish an approach using chamber-cultured sympathetic neurons (18), chimeric EGFR/Trk receptors (19), and EGF linked to Quantum dots (20) or to fluoro-nanogold (21), to specifically examine the dynamics, ultrastructure, and molecular composition of Trk-containing retrograde endosomes. By comparing Trk- to EGFR-mediated endosome axonal transport and somal signaling, we have elucidated key factors that uniquely define Trk endosome processing for sustained retrograde signaling.

Results

Paradigm for Trk Retrograde Signaling. To visualize Trk irrespective of p75NTR, we have used a chimeric EGFR/TrkB receptor (ETrkB) containing the extracellular domain of EGFR (22), activated by EGF-Quantum dot 605 (qEGF) (20). Treatment of PC12 cells with EGF or qEGF resulted in comparable activation of Erk1/2 (Fig. S1A). Both qEGF and ETrkB were specifically internalized into superior cervical ganglia (SCG) neurons expressing ETrkB and treated with 20 ng/mL qEGF (Fig. S1B). ETrkB and qEGF were highly colocalized (95.1% of qEGF puncta colocalized with ETrkB, $n = 143$), suggesting endocytosis of ligand/receptor complexes.

ETrkB endocytosis was selectively Pincher-dependent when compared in SCG neurons expressing either ETrkB or EGFR-GFP together with the dominant-negative PincherG68E. GFP-tagged EGFR is endocytosed and processed in the same manner as WT-EGFR (23). PincherG68E blocked EGF-mediated endocytosis of ETrkB, but EGFR endocytosis was unaffected (ETrkB endocytosed in no cells with PincherG68E, $n = 18$; EGFR-GFP endocytosed in 86.2% of cells with PincherG68E, $n = 29$, $P = 1.6 \times 10^{-9}$) (Fig. S1C). Electron microscopic (EM)

Author contributions: P.P., G.V., and S.H. designed research; P.P., G.V., and W.A. performed research; W.J.B. and H.J.F. contributed new reagents/analytic tools; P.P., W.A., and S.H. analyzed data; and P.P., G.V., and S.H. wrote the paper.

The authors declare no conflict of interest.

*This Direct Submission article had a prearranged editor.

¹Present address: The Howard Hughes Medical Institute, Smilow Neuroscience Program, New York University School of Medicine, New York, NY 10016.

²Present address: Department of Molecular and Cellular Biology, Harvard University, Cambridge, MA 02138.

³To whom correspondence should be addressed. E-mail: simon.halegoua@sunysb.edu.

This article contains supporting information online at www.pnas.org/lookup/suppl/doi:10.1073/pnas.1015981108/-DCSupplemental.

analysis verified that qEGF/ETrkB was selectively internalized in macroendosomes, at plasma membrane ruffles of hippocampal neurons ($n = 134$) (Fig. S2A); however, EGFR-GFP was rather found in qEGF-containing clathrin-coated pits and vesicles ($n = 40$) (Fig. S2B) but not macroendosomes, as reported for TrkA, TrkB, and EGFR (5, 8). No labeled clathrin-coated pits or vesicles were seen in ETrkB-expressing neurons and no labeled macroendosomes were seen in EGFR-expressing neurons.

Retrogradely Transported ETrkB-Signaling Endosomes Are MVBs. Retrogradely transported ETrkB endosomes were visualized in SCG somata grown in compartmentalized chambers after distal axons were treated with qEGF for 2 h (Fig. 1A). Briefly, SCGs were plated in compartmentalized chambers assembled on collagen-coated TC dishes. These chamber cultures, which effectively isolate the cell body from distal axons, are well used in NT retrograde-signaling studies (9, 18). Neurons were grown for about 10 to 14 d in order for their axons to extend to the side compartment and then infected with an ETrkB adenovirus. Adenovirus infection results in efficient gene transfer in chamber-cultured SCG neurons (7). After 48 h, cells were starved for 12 h in low-serum media and then treated with qEGF for 2 h at distal axons, washed, fixed, and processed for immunocytochemistry (*Materials and Methods*). Confocal analysis of immunostained ETrkB somata showed that most qEGF puncta were colabeled for ETrkB (86.5% $n = 74$) (Fig. 1B) and staining for Phospho-Erk indicated their association with active P-Erk (54%, $n = 160$) (Fig. 1B). These retrogradely transported Trk signaling endosomes, labeled by silver-enhanced qEGF, were exclusively MVBs ($n = 105$) (Fig. 1C), as evidenced by the existence of intraluminal vesicles in these endosomes.

ETrkB Retrograde Transport Requires Both Pincher and Rac. Rac and Pincher are uniquely required for Trk endocytosis in PC12 cells (5). To determine if Pincher- and Rac-mediated endosomes mediate ETrkB retrograde transport, we asked if dominant-negative forms of these proteins could block endosome accumulation in the soma, using a qEGF repeat-treatment paradigm (Fig. 2A). Chamber-cultured SCG neurons were infected with ETrkB adenovirus and after 2 d the distal axons treated with EGF conjugated to Qdot 525 (qEGF525) for 6 h. Three days later, cells were treated with qEGF605 for 2 h and somata were assessed for presence of qEGF525 and qEGF605. In these control cells, 65.7% of somata containing qEGF525 endosomal structures also contained qEGF605 endosomes ($n = 172$) (Fig.

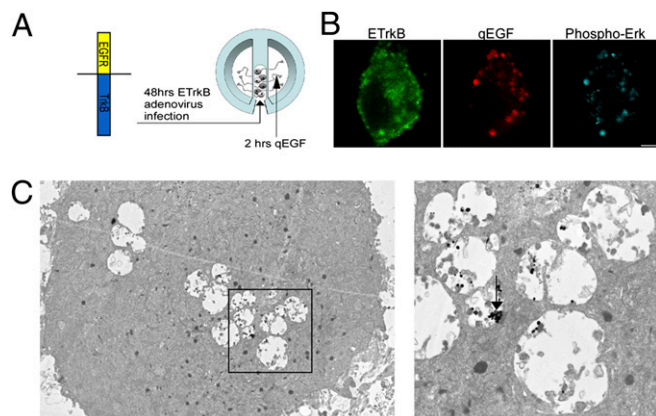


Fig. 1. Retrogradely transported ETrkB signaling endosomes are MVBs. (A) Distal axons of chamber-cultured SCGs infected with ETrkB adenovirus were treated with qEGF for 2 h. (B) Immunocytochemistry: ETrkB (anti-EGFR, green), qEGF (red), and phospho-Erk5 (anti-P-Erk5, cyan). (Scale bar, 2 μm .) (C) EM of soma shows silver-enhanced qEGF accumulated in partially filled MVBs (inset, arrow). (Scale bars, 500 nm.)

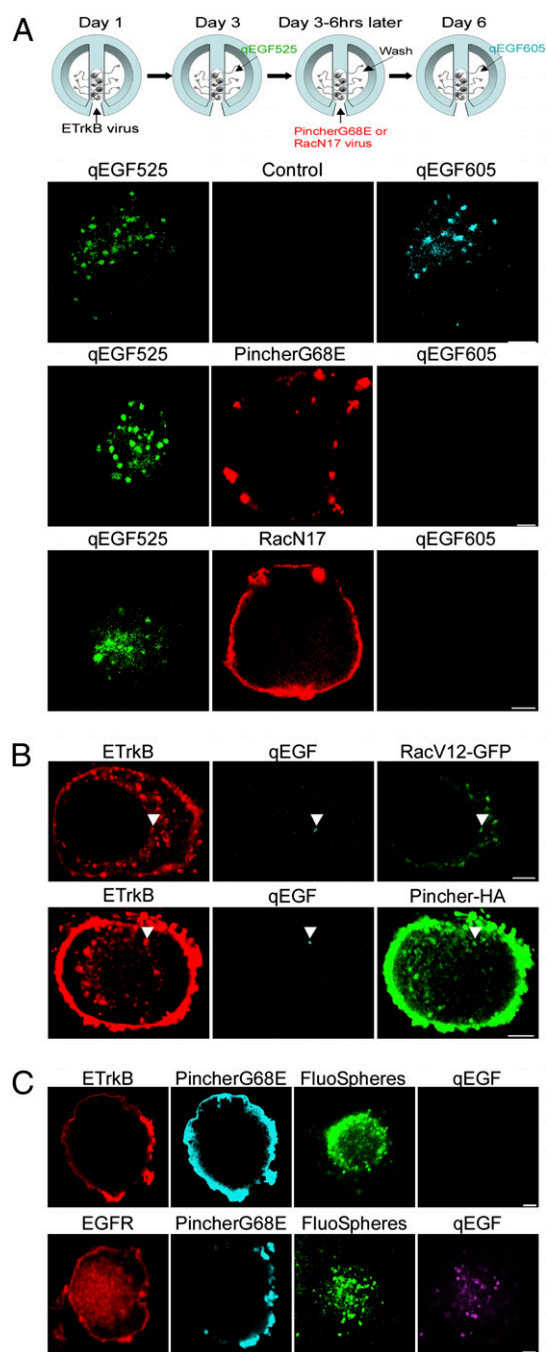


Fig. 2. ETrkB, but not EGFR, retrograde transport requires both Pincher and Rac functions. (A) Chamber-cultured SCG neurons were infected with ETrkB adenovirus, the distal axons treated with qEGF525 for 6 h and neurons infected with either PincherG68E-HA or RacN17-T7 adenoviruses for 3 d, and distal axons treated for 2 h with qEGF605 (see schematic). Immunocytochemistry: qEGF525 (green), qEGF605 (cyan), PincherG68E (anti-HA, red, *Top and Middle*), and RacN17 (anti-T7, red, *Bottom*). (B) Distal axons of chamber-cultured SCGs coinfecting with adenoviruses expressing ETrkB and either RacV12-GFP (*Upper*) or Pincher-HA (*Lower*) were treated with qEGF for 2 h. Immunocytochemistry: ETrkB (anti-EGFR, red), qEGF (cyan), RacV12-GFP (GFP, green, *Upper*) and Pincher-HA (anti-Pincher, green, *Lower*). Arrowheads point to receptor/qEGF complexes. (C) Distal axons of chamber-cultured SCGs coinfecting with adenoviruses expressing PincherG68E-HA or either ETrkB (*Upper*) or EGFR (*Lower*) were treated for 48 h with fluoSpheres and then with qEGF for 2 h. ETrkB (anti-EGFR, red, *Upper*), EGFR (anti-EGFR, red, *Lower*), PincherG68E (anti-Pincher, cyan), fluoSpheres (green), and qEGF (purple). (Scale bars, 2 μm .)

2A, Upper). To assess the requirements for Pincher or Rac in retrograde transport of qEGF, neurons were infected with adenoviruses expressing either PincherG68E or dominant-negative RacN17 during the 3 d between the qEGF525 and qEGF605 treatments. In neurons expressing PincherG68E or RacN17, qEGF was retrogradely transported in only 10.2% (85% block) or 32% (51% block) of the neuronal somata with qEGF525, respectively [$n = 88$, $P = 6.2 \times 10^{-25}$ for PincherG68E (Fig. 2A, Middle); $n = 72$, $P = 3.3 \times 10^{-8}$ for RacN17 (Fig. 2A, Lower)], indicating that both Pincher and Rac are required for Trk retrograde transport.

To determine if retrogradely transported Trk endosomes are derived from Rac- and Pincher-derived endosomes, chamber-cultured SCG neurons were coinfecting with ETrkB- and either constitutively active RacV12-GFP- or Pincher-HA-expressing adenoviruses and treated with qEGF at the distal axons. At least half of the ETrkB/qEGF complexes were associated with RacV12 (52.6%, $n = 211$) or Pincher (53.8%, $n = 91$), respectively, in the soma (Fig. 2B).

Differential Requirements for ETrkB and EGFR Retrograde Transport.

To determine if Pincher is selectively involved in Trk retrograde axonal transport, PincherG68E was coexpressed or not with either ETrkB or EGFR-GFP in adenovirus-infected, chamber-cultured SCG neurons and projecting neurons marked with fluoSpheres. After treating distal axons with qEGF for 2 h, retrograde transport was assessed as the percentage of fluoSphere-positive cells that showed appearance of qEGF at the soma: 78.3% of ETrkB-expressing neurons ($n = 152$) and 88.8% of EGFR-expressing neurons ($n = 116$) exhibited retrograde transport, but only 13.3% of ETrkB expressing neurons ($n = 45$ cells) as opposed to 83.3% ($n = 114$ cells) of EGFR expressing neurons exhibited retrograde transport when PincherG68E was coexpressed ($P = 1.3 \times 10^{-16}$) (Fig. 2C), indicating that Pincher is required for Trk, but not EGFR, retrograde transport.

Retrogradely Transported ETrkB and EGFR Endosomes Are Differentially Processed. We examined the association of retrogradely transported ETrkB and EGFR endosomes with the early and late endosomal markers Rab5 and Rab7. The distal axons of chamber-cultured SCG neurons expressing either ETrkB or EGFR together with either Rab5-GFP or Rab7-GFP were treated with qEGF for 2 h. Somal complexes of qEGF and ETrkB were found to be better associated with Rab5 (59.3%; $n = 273$) (Fig. 3A, Upper) than Rab 7 (34.8%; $n = 264$) (Fig. S3, Upper), but the reverse was true for complexes of qEGF and EGFR, more frequently associated with Rab7 (50.9%; $n = 266$) (Fig. 3A, Lower) than Rab5 (34.2%; $n = 222$) (Fig. S3, Lower) ($P = 3.0 \times 10^{-8}$).

To assess late-endosome/lysosomal processing, we compared the associations of both ETrkB and EGFR endosomes with the lysosomal marker cathepsin, again using the inorganic Qdot, which allowed us to follow the fate of the ligand (qEGF) even after ligand/receptor degradation in lysosomes. After treating distal axons of either ETrkB- or EGFR-expressing neurons with qEGF for 4 h, we found four categories of Qdot associations with ETrkB or EGFR endosomes in somata as follows: (i) qEGF associated with receptor but not cathepsin (51.8%, for ETrkB, 27.1% for EGFR), (ii) qEGF associated with both receptor and cathepsin (12.9% for ETrkB, 8.1% for EGFR), (iii) Qdot associated with cathepsin alone (13.4% for ETrkB, 36.4% for EGFR), and (iv) Qdot associated with neither receptor nor cathepsin (28.3% for ETrkB, 21.9% for EGFR). With ETrkB, the majority of qEGF was associated with receptor but not cathepsin (51.8%, $n = 224$), but only 27.1% ($n = 494$) of qEGF was associated with EGFR without cathepsin ($P < 0.0001$). In EGFR-expressing cells, qEGF was preferentially associated with cathepsin-containing structures, compared with ETrkB-expressing cells (44.5% vs.

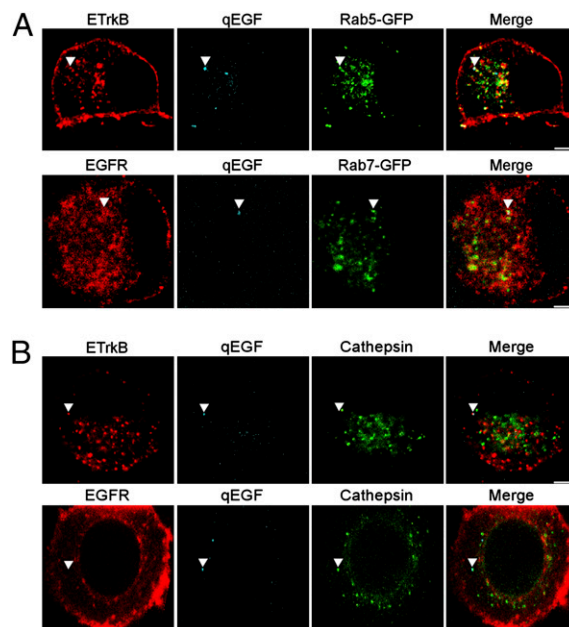


Fig. 3. Retrogradely transported ETrkB and EGFR endosomes are differentially processed by Rab5 and Rab7. Chamber-cultured SCG neurons were infected with either ETrkB (B, Upper) or EGFR (B, Lower) adenovirus alone, or also infected with either Rab5-GFP (A, Upper) or Rab7-GFP (A, Lower) adenovirus. After 2 d, the distal axons were treated with qEGF for 2 h (A) or 4 h (B). ETrkB (anti-EGFR, red, Upper), EGFR (anti-EGFR, red, Lower), qEGF (cyan), Rab5-GFP (GFP, green, A, Upper), Rab7 (GFP, green, A, Lower), and cathepsin (anti-cathepsin, green, B). Arrowheads point to receptor/qEGF complexes. (Scale bars, 2 μm.)

26.3%, respectively) (Fig. 3B). Colocalization of either receptor with cathepsin and qEGF was rarely seen, suggesting rapid receptor degradation at the lysosome.

We compared the ultrastructures of ETrkB and EGFR retrograde endosomes by EM, in which lysosomes appear as electron-dense structures. The distal axons of chamber-cultured SCG neurons expressing either receptor were incubated with qEGF for 2 h and the somata analyzed by EM. In ETrkB neurons, 70% of the qEGF-containing structures were electron-lucent MVBs and only 30% ($n = 105$) were electron-dense. However, in EGFR-expressing neurons, most of the qEGF was associated with electron-dense, lysosomal structures (61%, $n = 74$, $P = 0.03$) (Fig. 4A). Interestingly, proximal axons of EGFR-GFP-infected neurons displayed a high density of electron-dense lysosomes, contrary to the ETrkB-infected neurons that were essentially devoid of lysosomes (Fig. S4A). Furthermore, when a similar analysis was carried out in three-chamber neuronal cultures expressing EGFR, qEGF was found with electron-dense, lysosomal structures in the middle axonal chamber (Fig. S4B), suggesting lysosomal processing in axons.

We compared the temporal processing of ETrkB and EGFR into lysosomes using a pulse-chase paradigm. The distal axons of chamber-cultured SCG neurons expressing either ETrkB or EGFR were incubated with EGF coupled to 1-nm fluoro-nanogold particles (EGF-nG) for 30 min at 4 °C (pulse), the unbound EGF-nG was then removed, and the neurons reincubated at 37 °C (chase) for another 12 h before EM analysis with gold enhancement. As expected, the nG-containing structures in EGFR-expressing somata were often electron-dense (38%, $n = 52$) (Fig. S5). In contrast, the nG-containing structures in ETrkB expressing neurons were nearly devoid of lysosomal processing after the chase period (96% were electron lucent MVBs, $n = 54$; $P = 7.1 \times 10^{-6}$) (Fig. S5).

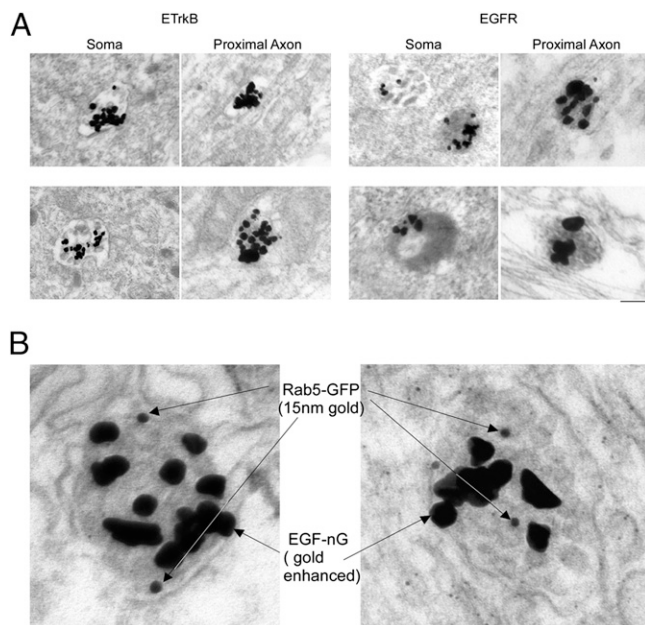


Fig. 4. ETrkB-MVBs retain Rab5. Chamber-cultured SCG neurons were (A) infected 48 h with an adenovirus expressing either ETrkB (Left) or EGFR (Right), the distal axons treated with qEGF for 2 h, and processed for silver-enhanced EM as in Fig. 2C (Scale bar, 200 nm), or (B) coinfecting 48 h with ETrkB and Rab5-GFP adenoviruses and distal axons treated 2 h with EGF-nG. (Scale bar, 50 nm.) Somata were processed for EM, with pre-embed gold-enhanced and postembedded immuno-gold-labeling for GFP. Two double-labeled MVBs are shown.

ETrkB MVBs Retain Rab5. To directly address the possibility of “immature” ETrkB-MVBs, we examined whether Rab5 was localized to retrogradely transported ETrkB-MVBs by double-labeling EM using EGF-nG, instead of qEGF, as the ligand. The distal axons of chamber-cultured SCGs expressing ETrkB and Rab5-GFP adenoviruses were treated with EGF-nG for 2 h. Fixed somata were gold-enhanced (to detect EGF-nG) and further processed for immuno-EM using anti-GFP antibody (to detect the Rab5-GFP). EGF-nG-containing MVBs were readily identified, which were immuno-positive for Rab5-GFP (Fig. 4B).

Retrogradely Transported ETrkB, but Not EGFR, Mediates Sustained Erk Signaling and Gene Induction. To investigate the signaling potential of each receptor/ligand complex, we first examined their association with activated, phospho-Erk. When distal axons of chamber-cultured SCG neurons expressing either ETrkB or EGFR-GFP were treated with qEGF for 2 h and immunostained with both anti-P-Erk5 and anti-EGFR antibodies, 53.7% ($n = 160$) of ETrkB/qEGF complexes were associated with phospho-Erk, as opposed to 32.6% ($n = 178$) of the EGFR/qEGF complexes (Fig. 5A) ($P = 1.1 \times 10^{-4}$).

To determine if Trk or EGFR would retrogradely mediate sustained somal Ras/Rap-Erk-CREB signaling, we assessed *vgf* gene expression (24, 25). Chamber-cultured SCG neurons were uninfected or EGFR adenovirus-infected, and the distal axons treated with NGF and fluoSpheres (to mark projecting neurons) or with qEGF for 10 h, respectively. NGF, but not qEGF, treatment caused an up-regulation of VGF in these neurons, seen by immunofluorescence (Fig. 5B). Of fluospheres-containing, NGF-treated neurons, 47% showed elevated VGF protein levels relative to untreated cells and normalized to cells with no fluoSpheres ($n = 76$). In contrast, no qEGF-containing cells showed increased VGF expression, relative to untreated and qEGF-lacking cells ($n = 42$, $P = 1.1 \times 10^{-8}$).

When Pincher function was blocked by retrograde infection of distal axons with a PincherG68E-Herpes Simplex Virus (HSV)-derived vector, only 27% of cells expressing PincherG68E showed elevated levels of VGF, as opposed to 93% of uninfected neurons and 90% of control GFP-HSV infected neurons ($n = 50$, $P = 4.3 \times 10^{-5}$) (Fig. 5C), demonstrating that NGF-induced retrograde gene induction is Pincher-dependent.

Discussion

Defining the precise characteristics of the retrograde axonal NT/Trk-signaling endosome has been hampered by technical limitations in directly tracking and distinguishing endosomes carrying Trk versus $p75^{NTR}$ receptors. We developed a unique paradigm in chamber-cultured neurons, using EGF-ligand bound to fluorescent and electron-dense nanoparticles, which circumvented this problem. We found that the retrogradely transported Trk receptor was delivered to the soma in a MVB, derived from Pincher- and Rac-dependent macroendocytosis. The Trk-MVB was refractory to Rab7 mediated lysosomal processing, thus sustaining the Erk signal needed to stimulate neuronal *vgf* gene expression.

Our paradigm exploited a chimeric TrkB receptor in which the NT-ligand binding domain was replaced with that for EGF (ETrkB), mitigating Trk signaling in response to EGF (19, 22). When expressed in chamber-cultured sympathetic neurons, ETrkB carried out endocytosis, retrograde axonal transport and sustained somal Erk signaling in response to EGF. Furthermore, the use of qEGF or EGF-nG enabled specific tracking of ETrkB/ligand complexes by both fluorescence and EM (20, 21). We distinguished the subset of Erk-activating, ligand-bound ETrkB receptors contained in MVBs derived from distal axons, thus positively identifying the MVB as the retrograde Trk-signaling endosome.

Although qEGF-ETrkB and qEGF-EGFR complexes were each retrogradely transported from axon to soma in MVBs, ETrkB endosomes were uniquely derived in a Pincher-dependent manner and retained Pincher during and after transport to the soma. ETrkB endosomes were derived from macroendocytosis, as illustrated by their cotransport with RacV12 and dependence on Rac function. Our findings are consistent with previous studies showing macroendocytic vs. clathrin-mediated endocytosis of Trk and EGFRs, respectively (5, 7, 8), and do not confirm a class of clathrin-derived Trk endosome (26).

The retrogradely transported ETrkB and EGFR endosomes were differentially processed. Both pulse-chase and steady-state analyses indicated that EGFR endosomes rapidly traversed into Rab7⁺ MVBs that fused with cathepsin-containing, electron-dense lysosomes, whereas similar processing of ETrkB endosomes was greatly attenuated. Lysosomal processing of endosomes appeared to begin at least in the proximal axon, where EGF-nG bound to EGFR, but not to ETrkB, was observed in these electron-dense structures. The retrograde ETrkB endosomes were Rab5⁺ MVBs, suggesting that the rate-limiting step for their late-endosome/lysosome processing lies in the exchange of Rab5 for Rab7 (27), regardless of MVB formation. Previously, the rate of lysosomal processing was found sensitive to manipulation of the ratios of Trk to Pincher, with a high ratio driving lysosomal processing (7). This finding is consistent with the present pulse-chase experiment, in which the lower receptor levels processed for endocytosis in the pulse showed a much slower rate of lysosomal processing. Our results indicate that Trk endosomes associate with Rab5 and Rab7 in a sequential manner influenced by time, receptor density, and cellular location during and after retrograde transport.

Retrogradely transported ETrkB endosomes had higher signaling efficacy than EGFR, as illustrated by their preferential association with activated Erk kinases. We showed that one outcome of the Trk-extended endosomal lifetime was the ability to selectively signal the stimulation of *vgf* neuropeptide gene expression, which requires sustained Erk-CREB signaling (24, 25) and should drive additional gene programs (2).

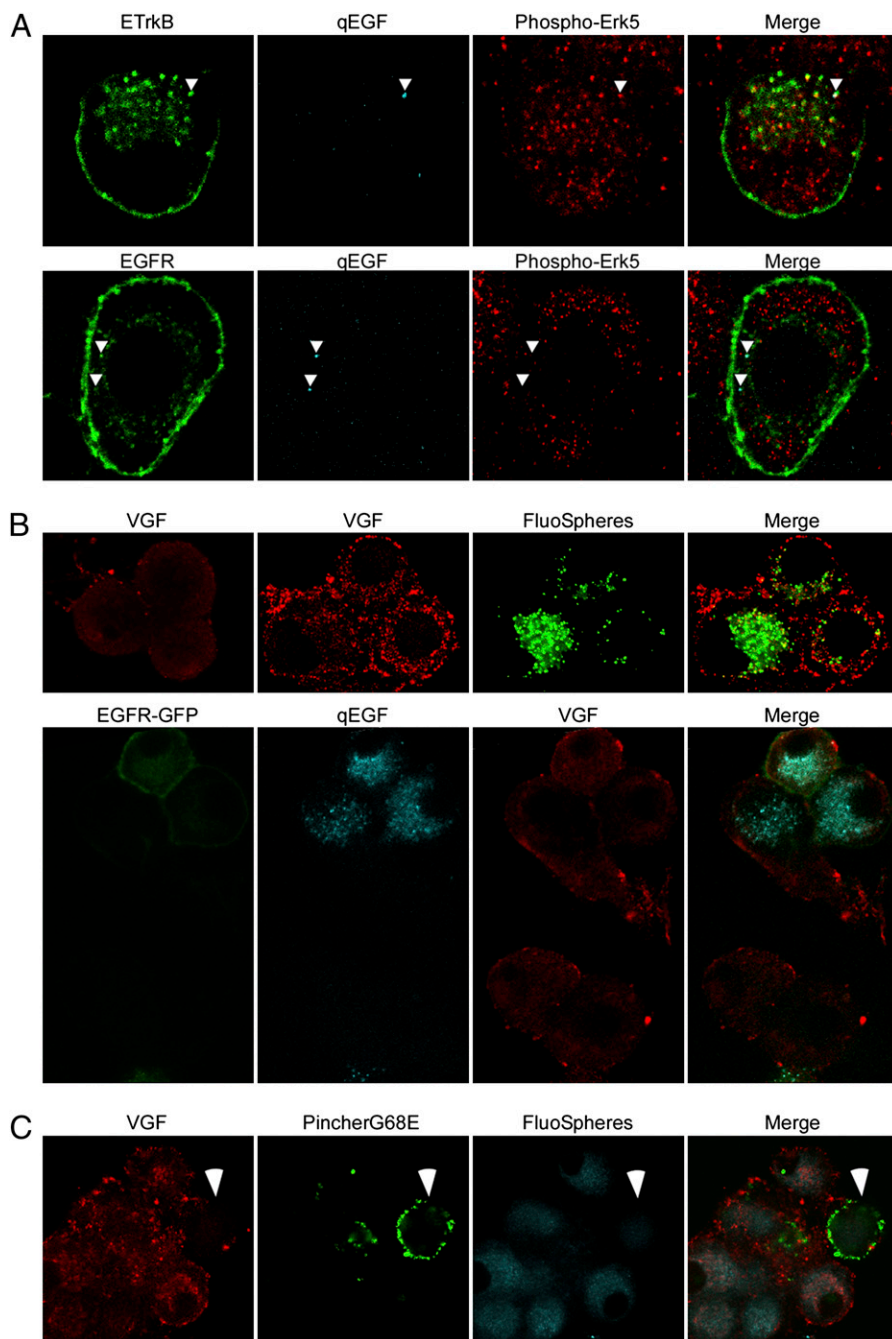


Fig. 5. Retrogradely transported endosomes containing ETrkB, but not EGFR, mediated sustained Erk signaling and *vgf* gene induction. Chamber-cultured SCG neurons were: (A) infected 48 h with either ETrkB (Upper) or EGFR (Lower) adenovirus, and the distal axon treated 2 h with qEGF. ETrkB (anti-EGFR, green, Upper), EGFR (anti-EGFR, green, Lower), qEGF (cyan), and phospho-Erk5 (anti-phospho-Erk5, red); arrowheads point to receptor/qEGF complexes; (B) untreated (Upper Left), treated at distal axons of uninfected (Upper), or EGFR-GFP adenovirus-infected (Lower) neurons with fluoSpheres and NGF (Upper Right) or qEGF alone (Lower) for 10 h, VGF (anti-VGF, red), fluoSpheres (green, Upper), EGFR-GFP (GFP, green, Lower), and qEGF (cyan, Lower); (C) NGF, starved for 48 h using anti-NGF and infected at distal axons with a PincherG68E-HSV and then treated for 10 h with fluoSpheres and NGF. VGF (anti-VGF, red), PincherG68E (anti-HA, green), and fluoSpheres (cyan). Arrowheads points to PincherG68E-expressing cell.

Our results favor a model in which endosome lifetime after retrograde transport dictates the endosomal capacity for the sustained signaling required to regulate neuronal gene expression. In this model, Pincher-mediated macroendocytosis generates Trk endosomes that are refractory to lysosomal processing, thus ensuring sustained endosomal signaling after retrograde transport to soma. Pincher-mediated macroendocytosis extends to retrograde signaling of antigrowth molecules (28), raising the possibility that Pincher may be generally used to generate long-lived endosomes required for sustained signaling paradigms.

Materials and Methods

Cell Culture. Dissociated rat SCG or hippocampal neurons were grown on collagen- or poly-d-lysine-coated TC dishes or on ACLAR (Ted Pella) or in compartmentalized chambers (CAMP 10 or CAMP 11; Tyler) (18) with 100 ng/mL NGF.

Growth Factors and Conjugates. Recombinant human EGF, EGF-biotin, streptavidin-Quantum dot (Qdot) 525 and 605 were from Invitrogen and streptavidin-fluoro-nanogold from Nanoprobes. EGF-biotin was coupled to either streptavidin-Qdot or fluoro-nanogold (20) and used at 80 ng/mL (active EGF concentration) at distal axons or 20 ng/mL at cell bodies.

Viral Vectors. Recombinant adenoviruses containing HA-Pincher and HA-PincherG68E (7), T7-RacN17, EGFR, ETrkB, EGFR-GFP, Rab5-GFP, Rab7-GFP, or RacV12-GFP were made using the Ad-Easy system (Stratagene). Recombinant adenoviruses containing HSVs containing PincherG68E or GFP were packaged into helper virus-free amplicon particles (29).

Western Blot Analysis. Blots of PC12 cell lysates were probed with rabbit antiphospho-erk1/2 antibody (1:500; Cell Signaling) and then anti-rabbit Alexa680 antibody (1:5,000; Invitrogen) (5), and developed using the Odyssey Infrared Imaging System (Version 2.1; Licor).

Immunofluorescence Staining and Confocal Microscopy. SCGs were infected with adenoviruses as indicated. After 48 h, neurons were NT-starved for 12 h in medium with 1% FBS. After EGF treatments, cells were washed with cold PBS, paraformaldehyde-fixed, and antibody-stained. Primary antibodies were rabbit anti-P-erk5 (1:500; Biosource), mouse-anti-HA (1:200; Santa Cruz Biotechnology), rabbit anti-Pincher (8) (1:1,000), mouse anti-T7 (1:400; Novagen), mouse anti-EGFR (1:100; Oncogene), goat anti-cathepsin (1:100; Santa Cruz), and rabbit anti-VGF (30) (1:750; S. Salton, Mount Sinai Medical Center, New York, NY). Secondary antibodies were donkey anti-mouse Alexa 488/Alexa 546 or donkey anti-rabbit-Alexa 488/Alexa 546 (Molecular Probes), goat anti-rabbit Cy5 or goat antimouse Cy5 (Jackson Labs). Images were obtained using a LSM 510 laser scanning confocal microscope (Zeiss). To avoid bleed-through, fluorophores were activated and signal captured sequentially using the following filters: 505–530/GFP/Alexa488, 560–610/Alexa546, and LP 650/Cy5.

Retrograde Transport and Signaling. SCGs grown in compartmentalized chambers for 8 to 10 d were double-infected with adenoviruses expressing PincherG68E and either ETrkB or EGFR-GFP and treated at distal axons for 48 h with yellow-green carboxylate modified microspheres (fluoSpheres, 1:1,000; Invitrogen), starved for 12 h, and then treated with qEGF for 2 h at the distal axons, fixed, and stained. Alternatively, chamber cultures were infected with an ETrkB adenovirus, starved, and then treated with qEGF525 for 6 h at the distal axons. After treatment, the distal axon compartments were washed and reinfected for 3 d with either RacN17-T7 or PincherG68E-HA adenoviruses, starved, and then treated with qEGF for 2 h at the distal axons, fixed, and stained. For VGF induction, SCGs in chamber cultures were starved 48 h with anti-NGF (1:10,000; Sigma), then treated with 100 ng/mL qEGF or NGF for 10 h, fixed, and stained for VGF. As indicated in the figure legends, at the time of starvation cells were infected either with an EGFR-GFP adenovirus or HA-PincherG68E HSV (applied at distal axons).

Electron Microscopy and Immunogold Labeling. Silver-enhanced Qdot. Neurons were fixed for 15 min in a mixture of cold 2% PFA and 2% glutaraldehyde in 0.1 M phosphate buffer (PB), pH 7.4, silver-enhanced (British Bio Cell; Ted Pella), postfixed with 1% osmium tetroxide, en bloc stained with 1% uranyl acetate, dehydrated, and embedded in Durcupan (Fluka). Ultrathin sections

(60–90 nm) were stained with 1% methanolic uranyl acetate and 0.3% aqueous lead citrate.

Gold-enhanced fluoro-nanogold. Cultured neurons were microwave fixed with cold 2% PFA and 0.1% glutaraldehyde in 0.1 M phosphate buffer (PB), pH 7.4, gold-enhanced (Nanoprobes), postfixed, stained, and embedded as usual. Serial ultrathin sections (60–90 nm) were cut on a Reichert Ultracut E ultramicrotome and picked up on formvar-coated nickel slot grids. Sections were postembbed immunogold-labeled for GFP within 24 h of sectioning (7, 8) and observed with a JEOL 1200EX transmission EM.

Image Processing and Quantitative Analysis. Fluorescence images were digitally analyzed using Aim 3.2 software (Carl Zeiss), processed using Photoshop (Adobe), and measured using Image J (National Institutes of Health). Endocytosis was scored positive when the ratio of total receptor cytoplasmic to membrane fluorescence intensities was greater than 1. For colocalization, the same channel gain settings were used for all images.

Qdots and receptor. Individual foci of endosomal Qdots were scored colocalized if they showed overlap of >90% with receptor. Colocalized Qdots with receptor were then further assessed for colocalization with endosomal markers. Data are an accumulation of all experiments (at least three chamber cultures per experiment).

VGF expression. Each cell was outlined and the average pixel intensity for that area calculated using ImageJ. Baseline VGF expression was defined by the average fluorescence intensities of all untreated (control) cells. Cells with higher average fluorescence intensity than this baseline were scored as induced.

Statistical Analysis. The two-tailed Fisher's Exact Test was used and verified using the χ^2 test.

ACKNOWLEDGMENTS. We thank J. Rosenbaum (Stony Brook University, Stony Brook, NY) for technical assistance, L. Lotta and C. Burris (University of Rochester, Rochester, NY) for Herpes Simplex Virus packaging, S. Salton (Mount Sinai Medical Center, New York, NY) for anti-VGF antibody, and X. Tu and N. Mendell (Stony Brook University, Stony Brook, NY) for statistical analyses. This work was supported in part by National Institutes of Health Grants NS18218 (to S.H.) and U54-NS045309 (to H.J.F. and W.J.B.).

- Levi-Montalcini R (1987) The nerve growth factor 35 years later. *Science* 237:1154–1162.
- Zweifel LS, Kuruvilla R, Ginty DD (2005) Functions and mechanisms of retrograde neurotrophin signalling. *Nat Rev Neurosci* 6:615–625.
- Halegoua S, Armstrong RC, Kremer NE (1991) Dissecting the mode of action of a neuronal growth factor. *Curr Top Microbiol Immunol* 165:119–170.
- Beattie EC, et al. (1996) A signaling endosome hypothesis to explain NGF actions: Potential implications for neurodegeneration. *Cold Spring Harb Symp Quant Biol* 61:389–406.
- Valdez G, et al. (2007) Trk-signaling endosomes are generated by Rac-dependent macroendocytosis. *Proc Natl Acad Sci USA* 104:12270–12275.
- Daumke O, et al. (2007) Architectural and mechanistic insights into an EHD ATPase involved in membrane remodelling. *Nature* 449:923–927.
- Valdez G, et al. (2005) Pincher-mediated macroendocytosis underlies retrograde signaling by neurotrophin receptors. *J Neurosci* 25:5236–5247.
- Shao Y, et al. (2002) Pincher, a pinocytic chaperone for nerve growth factor/TrkA signaling endosomes. *J Cell Biol* 157:679–691.
- Ye H, Kuruvilla R, Zweifel LS, Ginty DD (2003) Evidence in support of signaling endosome-based retrograde survival of sympathetic neurons. *Neuron* 39(1):57–68.
- Watson FL, et al. (2001) Neurotrophins use the Erk5 pathway to mediate a retrograde survival response. *Nat Neurosci* 4:981–988.
- Delcroix JD, et al. (2003) NGF signaling in sensory neurons: Evidence that early endosomes carry NGF retrograde signals. *Neuron* 39(1):69–84.
- Cui B, et al. (2007) One at a time, live tracking of NGF axonal transport using quantum dots. *Proc Natl Acad Sci USA* 104:13666–13671.
- Deinhardt K, et al. (2006) Rab5 and Rab7 control endocytic sorting along the axonal retrograde transport pathway. *Neuron* 52:293–305.
- Schwab ME (1977) Ultrastructural localization of a nerve growth factor-horseradish peroxidase (NGF-HRP) coupling product after retrograde axonal transport in adrenergic neurons. *Brain Res* 130(1):190–196.
- Claude P, Hawrot E, Dunis DA, Campenot RB (1982) Binding, internalization, and retrograde transport of 125 I-nerve growth factor in cultured rat sympathetic neurons. *J Neurosci* 2:431–442.
- Bronfman FC, Tcherpakov M, Jovin TM, Fainzilber M (2003) Ligand-induced internalization of the p75 neurotrophin receptor: A slow route to the signaling endosome. *J Neurosci* 23:3209–3220.
- Hibbert AP, Kramer BM, Miller FD, Kaplan DR (2006) The localization, trafficking and retrograde transport of BDNF bound to p75NTR in sympathetic neurons. *Mol Cell Neurosci* 32:387–402.
- Campenot RB (1977) Local control of neurite development by nerve growth factor. *Proc Natl Acad Sci USA* 74:4516–4519.
- Obermeier A, et al. (1993) Tyrosine 785 is a major determinant of Trk—Substrate interaction. *EMBO J* 12:933–941.
- Lidke DS, et al. (2004) Quantum dot ligands provide new insights into erbB/HER receptor-mediated signal transduction. *Nat Biotechnol* 22:198–203.
- Takizawa T, Robinson JM (2000) FluoroNanogold is a bifunctional immunoprobe for correlative fluorescence and electron microscopy. *J Histochem Cytochem* 48:481–486.
- Wang JK, Xu H, Li HC, Goldfarb M (1996) Broadly expressed SNT-like proteins link FGF receptor stimulation to activators of Ras. *Oncogene* 13:721–729.
- Carter RE, Sorkin A (1998) Endocytosis of functional epidermal growth factor receptor-green fluorescent protein chimera. *J Biol Chem* 273:35000–35007.
- D'Arcangelo G, Habas R, Wang S, Halegoua S, Salton SR (1996) Activation of codependent transcription factors is required for transcriptional induction of the vgf gene by nerve growth factor and Ras. *Mol Cell Biol* 16:4621–4631.
- D'Arcangelo G, Halegoua S (1993) A branched signaling pathway for nerve growth factor is revealed by Src-, Ras-, and Raf-mediated gene inductions. *Mol Cell Biol* 13:3146–3155.
- Howe CL, Valletta JS, Rusnak AS, Mobley WC (2001) NGF signaling from clathrin-coated vesicles: Evidence that signaling endosomes serve as a platform for the Ras-MAPK pathway. *Neuron* 32:801–814.
- Rink J, Ghigo E, Kalaidzidis Y, Zerial M (2005) Rab conversion as a mechanism of progression from early to late endosomes. *Cell* 122:735–749.
- Joset A, Dodd DA, Halegoua S, Schwab ME (2010) Pincher-generated Nogo-A endosomes mediate growth cone collapse and retrograde signaling. *J Cell Biol* 188:271–285.
- Bowers WJ, Howard DF, Brooks AI, Halterman MW, Federoff HJ (2001) Expression of vhs and VP16 during HSV-1 helper virus-free amplicon packaging enhances titers. *Gene Ther* 8(2):111–120.
- Levi A, Ferri GL, Watson E, Possenti R, Salton SR (2004) Processing, distribution, and function of VGF, a neuronal and endocrine peptide precursor. *Cell Mol Neurobiol* 24:517–533.